

# Photonic circuits based on Mach Zehnder interferometer (MZI): A paradigm shift in solar irradiance studies

Adriany R. Barbosa<sup>\*a</sup>, Franciele Carlesso<sup>a</sup>, Igor Y. Abe<sup>b</sup>, Marco I. Alayo<sup>b</sup> e Luís Eduardo A. Vieira<sup>a</sup>

<sup>a</sup> INPE - National Institute for Space Research, Av. dos Astronautas, 1.758 - Jardim da Granja, São José dos Campos - SP, Brazil 12227-010; <sup>b</sup> USP - University of Sao Paulo, Av. Prof. Luciano Gualberto, 158 - Butantã, São Paulo - SP, Brazil 05508-010

## ABSTRACT

The Total Solar Irradiance (TSI) is the principal energy source that propels dynamic changes within the Earth's climate system over extended periods. The variability in TSI plays a crucial role in shaping the long-term evolution of the Earth's climate. This study proposes to introduce a novel approach to investigating irradiation and advancing our understanding of solar radiation's impact on Earth's climate by leveraging circuit technology. Photonic integrated circuits (PICs) represent a pioneering breakthrough in integrating multiple optical components. In contrast to existing sensor platforms, PICs offer increased sensitivity, less interference from electromagnetic noise in measurements, and a more compact design. Most instruments in space that measure TSI are called electrical substitution radiometers (ESR). An ESR usually includes an optical absorbing element connected to a reference heat sink. A poorly conducting thermal link keeps the heat sink at a constant temperature. The instrument compares the heating caused by the radiant power absorbed with the heating caused by an electrical current. The Brazilian National Institute for Space Research (INPE) has initiated a project to create solar observational tools as part of the global effort to comprehend the workings of the Sun and its impact on Earth. The Galileo Solar Space Telescope (GSST) comprises two instrument designs - Irradiance Monitor Module (IMM) - to accomplish the mission objectives. One of the tools is a small radiometer constructed on a photonic integrated circuit. The primary objective of this research is to mitigate instrument uncertainty and elevate temperature measurement techniques in radiometers. By exploring innovative ideas and approaches, this work seeks to redefine state-of-the-art temperature quantification within these crucial scientific instruments. A key aspect of our methodology involves implementing a new instrument design utilizing Mach Zehnder Interferometer (MZI) technology embedded in a substrate for temperature detection. Adopting photonic circuits is a pivotal strategy to provide a more direct and durable solution to temperature sensing. This approach is anticipated to minimize uncertainties associated with electronics and comparators. Here, we will showcase the results of the preliminary manufacturing outcomes. These findings contribute to the ongoing efforts to enhance temperature measurement techniques, aiming to deepen our comprehension of how the Sun's energy influences Earth. Through this work, we anticipate advancing the capabilities of radiometric instruments and paving the way for a more nuanced understanding of the Sun and climate dynamics.

**Keywords:** Total Solar Irradiance (TSI), Climate Variability, Photonic Integrated Circuits (PICs), Mach Zehnder Interferometer (MZI), Temperature Sensor, GSST

## 1. INTRODUCTION

Solar irradiance, quantified as Total Solar Irradiance (TSI), plays a pivotal role in shaping Earth's climatic dynamics. As the principal driving energy source in Earth's system, variations in solar radiation are the most widely acknowledged mechanism through which the Sun influences Earth's climate. The radiant power from the Sun is measured as the total solar energy reaching the Earth's upper atmosphere per unit area and standardized to one astronomical unit (AU) <sup>1-3</sup>.

The TSI exhibits fluctuations over various timescales due to several factors, predominantly phenomena within the Sun's surface, the photosphere <sup>4,5</sup>. One significant contributor to TSI variation is the presence of sunspots, dark patches on

the photosphere caused by intense magnetic activity. These sunspots arise from the complex interplay of the Sun's magnetic field lines, which can inhibit the outward flow of energy, leading to localized cooling and, thus, a decrease in TSI <sup>6</sup>.

Besides sunspots, solar faculae also play a role in TSI fluctuations. Faculae are patches that emerge on the Sun's surface around sunspots and are linked to regions with heightened magnetic activity. Unlike sunspots, faculae are brighter and hotter than their surroundings <sup>7</sup>. They form due to field concentrations that impede energy transfer, allowing the underlying plasma to rise closer to the surface. This increases radiation emission from the photosphere around them, contributing to the energy output <sup>8</sup>.

The connection between the Earth's climate and the Sun has been a research subject for years, and our knowledge has advanced. In the 1800s, a British astronomer named William Herschel made one of the discoveries associating solar behavior with climate patterns. Herschel noticed a link between decreased sunspot activity periods of activity and cooler temperatures on Earth. This discovery raised the possibility that changes in energy output and total solar irradiance could impact the Earth's climate <sup>9</sup>. However, in 1976, this info gained new light by a paper by Eddy (1976). Eddy showed the relationship between the Maunder Minimum and the Little Ice Age in Europe in this paper. Further investigations throughout the 19th and 20th centuries provided additional evidence supporting the idea of a solar-climate connection <sup>2,11,12</sup>. Additionally, studies of proxy climate data, such as ice cores and tree rings, revealed long-term climate trends that appeared to align with variations in solar activity <sup>13</sup>.

However, it is crucial to emphasize that solar variability is just one factor that shapes Earth's climate system. Earth's climate is also greatly influenced by other elements, such as greenhouse gas concentrations, volcanic activity, ocean circulation patterns, and human activity <sup>14</sup>.

Understanding the role of solar activity in Earth's climate system is crucial for distinguishing between natural climate fluctuations and those influenced by human-induced climate change. By integrating historical solar irradiance data with climate records, researchers can estimate the contribution of solar variability to observable climate changes. This analysis not only validates climate modeling and forecasting efforts but also provides valuable insights for predicting future climate patterns, thereby aiding in our collective efforts to mitigate and adapt to climate change <sup>14</sup>.

The field of TSI monitoring, which has been challenging with observational difficulties, has seen significant advancements since 1978. Space-born TSI measuring instruments, called Electrical Substitute Radiometers (ESR), consist of an optical absorbing element linked to a reference heat sink <sup>15-17</sup>. These instruments, most of which use absorber cavities to enhance radiation trapping efficiency, have provided continuous measurements, improving our understanding of TSI variance <sup>18</sup>.

ESRs measure the TSI by using electrical circuits to balance the heating effect of the incoming solar radiation <sup>16</sup>. It measures electrical power to keep the detector temperature constant during modulated incident radiation. Two cavities, one active and another serving as a thermal reference, are housed at the same temperature. These cavities are coated with an optical absorbing element with high absorbance, efficiently converting incident radiation into heat. A resistive heater circuit maintains a constant amount of Joule heat in the reference sensor, elevating it to a specific temperature. The active sensor is driven to the same temperature via a servo system, ensuring thermal balance. When the shutter opens, incident light enters the active cavity. Thus, the electrical heat to the active sensor is reduced, effectively substituting it with radiant energy. Accurate knowledge of electrical heating allows for precise measurement of the heating effect of solar radiation, which is proportional to the TSI <sup>19</sup>.

Over time, radiometers have been refined through various improvements, such as using more suitable absorber materials, modifications to cavity geometries, precision aperture designs, and an increased number of cavities. These improvements were made to monitor degradation and reduce measurement uncertainties more accurately <sup>18</sup>.

The continuous monitoring of TSI, crucial for capturing its dynamic behavior accurately, necessitates the development of advanced tools designed explicitly for TSI monitoring. The demand for such instruments has increased due to the need for higher data resolution and more frequent monitoring. Compact equipment for TSI measurement provides several advantages, including simplified deployment, cost reduction, and lower power and weight requirements. This underscores the need for more advanced tools that can accurately and consistently measure the TSI, driving the development of new technologies in the field <sup>4,18</sup>.

ESRs have limitations despite radiometer advancements. A key issue is the discrepancy between measured optical power and Joule heat due to differences in radiant and electric heat flux distributions. Ambient-temperature ESRs also suffer from low sensitivity and high thermal inertia, making them prone to overheating and affecting electronic circuit performance. Additionally, thermal noise limits the signal-to-noise ratio when monitoring low-level radiant fluxes, reducing sensitivity for accurate spectral assessment of thermal radiation sources like the Sun<sup>17,20</sup>.

Temperature sensors are vital in accurately measuring TSI, as temperature variation is directly related to the incident solar energy<sup>21,22</sup>. Currently, commercial thermistors are the most commonly used devices for these occasions. However, they have limitations, such as limited sensitivity, nonlinear response, and susceptibility to electromagnetic interference, which can compromise precision accuracy<sup>23</sup>.

In 2014, the National Institute for Space Research (INPE) launched the Galileo Solar Space Telescope (GSST) program to advance solar observation instruments for solar-terrestrial physics research<sup>24</sup>. The GSST is Brazil's first solar mission to conduct high-resolution solar observations. It seeks to explore the outer layer of the Sun's magnetic structures, the Sun's influence on Earth's climate, and its effects on Geospace. The mission is structured into three phases. The payload package includes high-resolution telescopes with spectropolarimeters in visible and ultraviolet wavelengths, an absolute radiometer, a particle detector, and a magnetometer. The instrument roadmap outlines the development from ground prototypes to formal space system development, incorporating innovative solutions and rigorous testing<sup>18,25-29</sup>. Despite advancements in radiometer technology, understanding long-term Total Solar Irradiance (TSI) variability and its implications remains incomplete. TSI fluctuations attributed to surface magnetic alterations are a well-established mechanism. Therefore, integrating an absolute radiometer is essential to complement the GSST spectropolarimeters' data, enabling a deeper understanding of the physical phenomena governing solar activity and irradiance variability. Recognizing the design limitations of the ESR, the team is exploring alternative thermo-optic sensors utilizing a Mach-Zehnder interferometer (MZI) based on refractive index variations in materials, offering potential improvements in efficiency and performance<sup>18</sup>.

Photonic Integrated Circuits (PICs) have emerged as a game-changer in various technological domains, ushering in a new era of compact, efficient, and high-performance optical systems. These integrated circuits are not just revolutionizing industries from telecommunications to healthcare, but also enabling unprecedented advancements in data transmission, sensing, and imaging. In sensing, PICs offer distinct advantages such as enhanced sensitivity, reduced size, and scalability, making them particularly valuable for applications demanding precision and reliability. Their ability to integrate multiple optical functions on a single chip opens up possibilities for the development of multifunctional and highly integrated sensor platforms, setting new standards for sensitivity, speed, and versatility. As the demand for sophisticated sensing solutions continues to grow across diverse sectors, the role of PICs is set to become increasingly pivotal in driving innovation and addressing complex challenges in the modern world<sup>32-34</sup>.

The MZI relies on total internal reflection for light confinement, splitting, and recombining laser beams at a Y-junction. Ideally, an MZI has no losses due to attenuation or radiation; when both interferometer arms have identical optical paths, the input and output light are in phase<sup>35</sup>.

However, altering the refractive index in one arm changes its optical path. This can be achieved by adjusting pressure or temperature above the waveguide core or using liquids with varying refractive indices. The phase difference at the MZI's final section causes interference, affecting the device's output power<sup>35-38</sup>.

MZIs have been used as pressure sensors<sup>39</sup>, biosensors<sup>40,41</sup>, and thermo-electro-optic sensors<sup>38</sup>. In radiometers, radiation absorption in one MZI arm changes the refractive index due to temperature variation, causing interference and enabling radiant flux computation through PID control.

Despite challenges like device length, MZI design could enhance temperature detection accuracy, reduce radiometer size and costs, and monitor TSI variations over extended periods. Improving instrument sensitivity and stability is crucial for understanding the Sun's impact on Earth's climate, requiring precise and stable solar irradiance data for reliable climate and atmospheric models<sup>13,14,42,43</sup>.

This paper seeks to investigate the capabilities of photonic circuits employing the Mach-Zehnder interferometer as a transformative approach in solar irradiance research. We will elaborate on the fabrication method employed for these state-of-the-art sensors and introduce preliminary findings.

## 2. METHODS

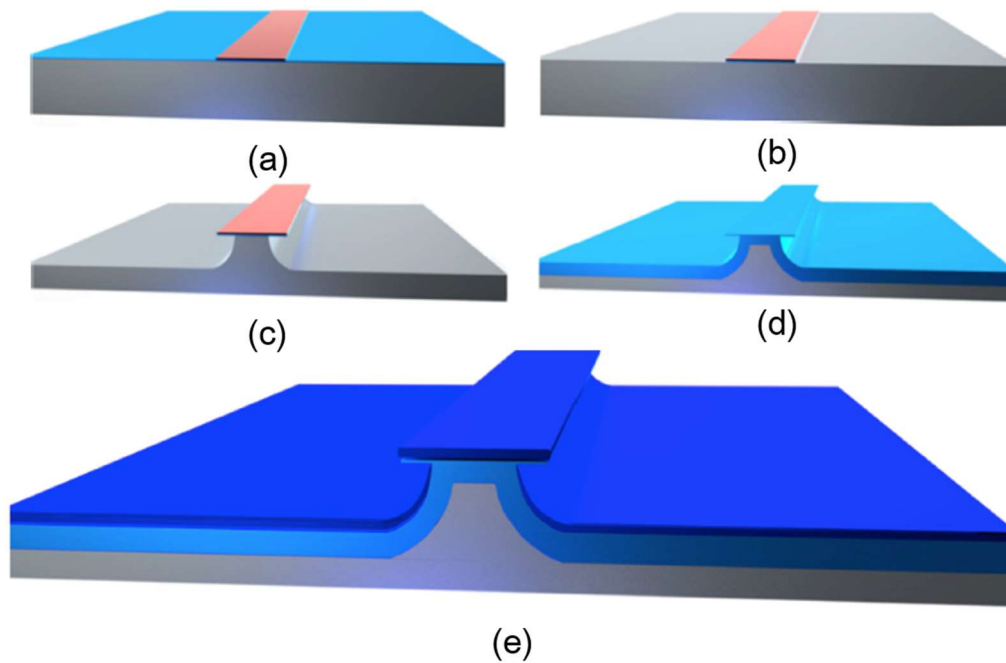


Figure 1: Diagram of the pedestal waveguide manufacturing process. a) SiO<sub>2</sub> film growth and photoresist application: Start with the growth of the SiO<sub>2</sub> film on the silicon substrate and application of photoresist, followed by photolithography to define the waveguides. b) Wet etching of SiO<sub>2</sub>: Buffered oxide etching (BOE) solution is used to etch SiO<sub>2</sub>, forming the basic structure of the guides. c) Dry etching of the silicon to form the pedestal d) Removal of the silicon substrate's photoresist and wet oxidation: Cleaning the photoresist and subsequent wet oxidation to prepare the surface for the next step. e) Deposition of the core material: Finalization is done with the material that will constitute the waveguide's core; in this work, Tantalum Pentoxide (Ta<sub>2</sub>O<sub>5</sub>) was used<sup>44</sup>.

The first step in the process is cleaning the silicon wafers. They undergo a thorough RCA-1 cleaning process to remove any organic residues. During this process, the silicon is oxidized, leaving a thin oxide layer on the surface of the wafer. This layer is then removed. After cleaning, the silicon samples are subjected to dry thermal oxidation, resulting in the formation of a relatively thick silicon dioxide film, which is about 150-200 nm thick. The refractive index of this film is 1.46<sup>45-47</sup>.

During the process of lithography (Fig. 1a), several steps were taken with the silicon wafers. Firstly, the hexamethyldisiloxane adhesion promoter was applied by spin-coating. Then, ma-N 1405, a negative photoresist, was spin-coated onto the wafers. The photoresist was then sensitized using a 385 nm laser in the MicroWriter ML3, which is a direct-write photolithography machine employed for the MZI geometry. After this, the wafers underwent post-exposure and were developed by a ma-D 533S developer. The final step of lithography was a hard bake.

The lithography mask utilized in the project was created with the help of CleWin Lithography Mask Design Software. This software provides easy modification options through scripting, which makes it possible to customize the device's line width, spacing between arms, and the radius of curvature for the S-bends with precision. Such a high level of adaptability is essential for designing the MZI to function as either a thermal sensor or an electro-optical modulator.

The process began with wet etching of the silicon dioxide layer by immersing the samples in a buffered oxide etch (BOE) solution (Fig. 1b). Then, dry etching of silicon was performed using sulfur hexafluoride (SF<sub>6</sub>) plasma etching to create the pedestal structure (Fig. 1c). Following the dry etching, a secondary cleaning was carried out to eliminate any residual photoresists and contaminants from the samples.

The silicon samples underwent a second round of thermal oxidation to grow an additional silicon dioxide layer, about 2-3  $\mu\text{m}$  thickness (Fig. 1d). For the core deposition, tantalum pentoxide ( $\text{Ta}_2\text{O}_5$ ) was used, and a tantalum target of 99.9% purity was employed for reactive DC sputtering (Fig. 1e). The resulting material had a thickness of 250 nm and exhibited a refractive index ranging from 2.1 at 633 nm.

A significant advantage of pedestal waveguides lies in eliminating post-core deposition etching, streamlining the fabrication process, and potentially augmenting device robustness. Pedestal waveguides exhibit distinct structural characteristics that differentiate them from conventional rib waveguides, predominantly concerning propagation losses. In pedestal waveguides, the mode is enveloped by deposited sidewalls instead of etched sidewalls in rib waveguides, resulting in attenuated losses. This reduced interaction between the mode and the sidewalls of the pedestal contributes to the diminished losses observed. Additionally, pedestal waveguides provide flexibility in selecting core materials, accommodating optical materials that are traditionally challenging to etch. Such adaptability not only expands the repertoire of available materials but also can reduce losses relative to rib waveguides<sup>46,47</sup>.

### 3. RESULTS

This study provides a thorough examination of the Mach-Zehnder Interferometer (MZI) through the use of optical and scanning electron microscopy (SEM). The study aims to present the structural details of the MZI and provide a better understanding of its optical properties.

Figure 2 illustrates the MZI's layout, showing the waveguides and 'S-bend' connections. The MZI's length (L) measures 15 mm, with a distance (D) of 0.5 mm between its arms. The design features an 'S-bend' structure with a radius of curvature set at 3.2 mm, and the waveguide thickness is 1  $\mu\text{m}$ . These details are crucial to the MZI's performance and contribute to the device's optical response.

Figure 3 provides a scanning electron microscopy image of the MZI's waveguide's pedestal structure, giving a cross-sectional view. The image shows the distinct layers (Substrate: Si, Cladding:  $\text{SiO}_2$ , and Core:  $\text{Ta}_2\text{O}_5$ ) and pedestal configuration, providing insight into the optical properties of the device. The pedestal structure plays a critical role in the MZI's performance, and understanding its characteristics is essential to optimizing the device's functionality.

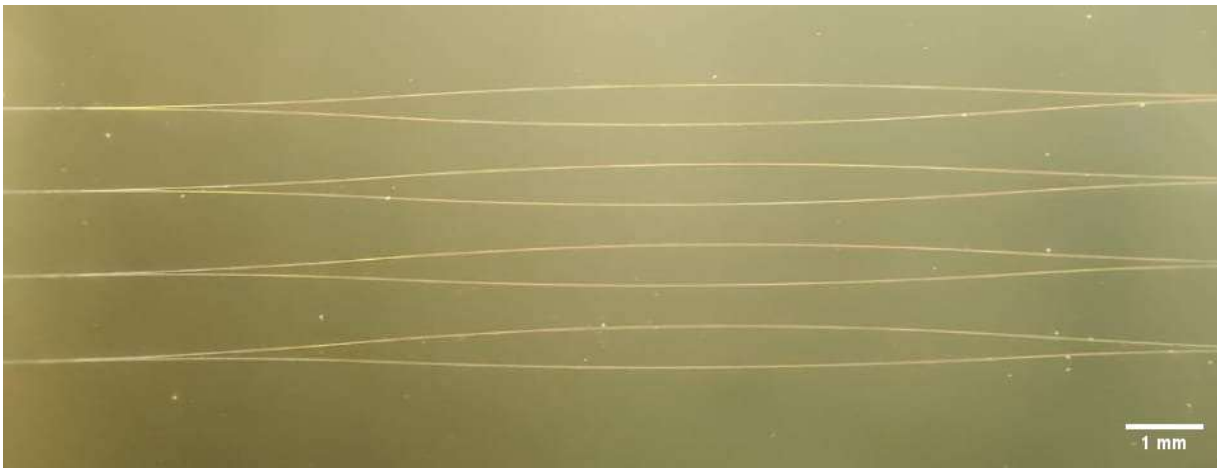


Figure 2: Optical microscope image of the complete MZI structure.

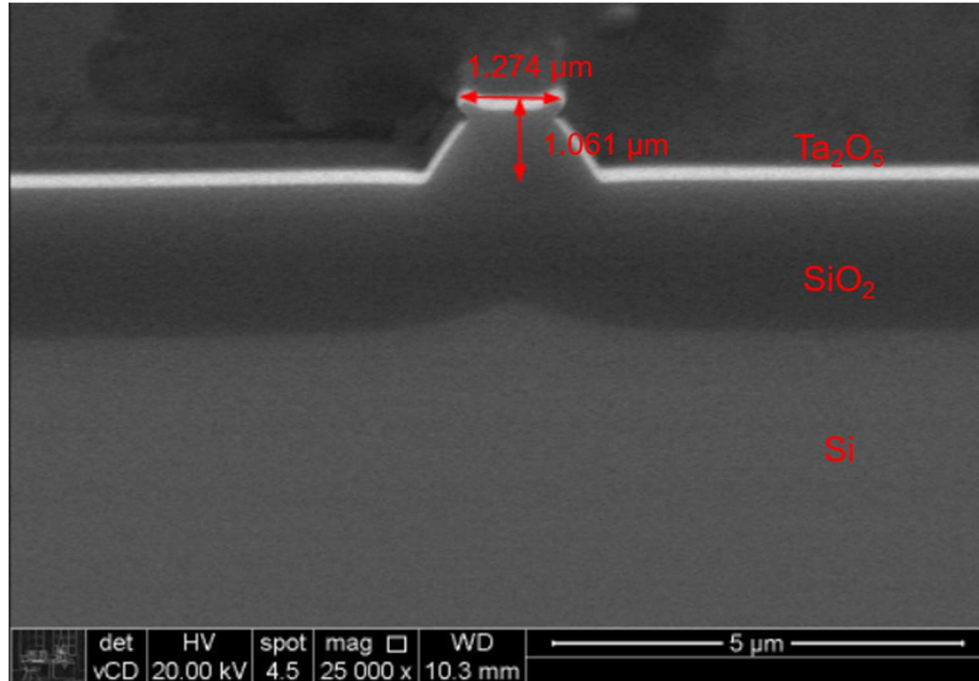


Figure 3. Scanning Electron Microscopy (SEM) of the cross section of the pedestal structure of the waveguide, showing the distinct layers and the pedestal configuration.

#### 4. NEXT STEPS

In the next phase of our work, we will focus on characterizing the waveguides to enhance their performance. First, we aim to optimize the transmission efficiency by fine-tuning the manufacturing parameters to minimize losses. This will involve evaluating the coupling efficiency at the input and output interfaces to ensure optimal light propagation through the device. Additionally, we will assess the insulation layer between the interferometer arms, examining its thermal conductivity, mechanical stability, and environmental resilience to ensure reliable performance under various conditions.

Furthermore, we plan to introduce an absorbent material into one of the interferometer arms to enhance its functionality. To achieve this, we will develop a deposition strategy tailored to deposit the absorbent material uniformly. We will optimize the deposition process to ensure consistent coating thickness and reproducible results, aiming to improve the device's overall sensitivity and performance.

#### 5. CONCLUSION

In conclusion, this study delves into developing a prototype Mach-Zehnder Interferometer-based sensor for temperature detection. The primary objective is to deepen our understanding of the Sun's impact on Earth's climate by accurately measuring temperature variations. Preliminary findings indicate promising feasibility for manufacturing the Mach-Zehnder device utilizing monomodal pedestal-style waveguides. These encouraging results lay a robust groundwork for subsequent investigations, paving the way for advancements in sensor technology and climate research.

#### ACKNOWLEDGEMENTS

The authors would like to thank Coordenação de Aperfeiçoamento de Pessoal de Nível Superior (CAPES), Conselho Nacional de Desenvolvimento Científico e Tecnológico (CNPq) (grant 141449/2021-7) and Fundação de Amparo à Pesquisa do Estado de São Paulo (FAPESP) (grant 2023/01324-6) for the financial support during the execution of this work.

## REFERENCES

- [1] Kopp, G., “Magnitudes and timescales of total solar irradiance variability,” *Journal of Space Weather and Space Climate* **6**, 1–11 (2016).
- [2] Solanki, S. K., Krivova, N. A. and Haigh, J. D., “Solar irradiance variability and climate,” *Annu Rev Astron Astrophys* **51**, 311–351 (2013).
- [3] Marchenko, S. V., Lean, J. L. and DeLand, M. T., “Relationship between Total Solar Irradiance and Magnetic Flux during Solar Minima,” *Astrophys J* **936**(2), 158 (2022).
- [4] Fröhlich, C. and Lean, J., “Solar radiative output and its variability: Evidence and mechanisms,” *Astronomy and Astrophysics Review* **12**(4), 273–320 (2004).
- [5] Schmutz, W. K., “Changes in the Total Solar Irradiance and climatic effects,” *Journal of Space Weather and Space Climate* **11** (2021).
- [6] Solanki, S. K., “Sunspots: An overview,” *Astronomy and Astrophysics Review* **11**(2–3), 153–286 (2003).
- [7] Solov’ev, A. A. and Kirichek, E. A., “Structure of solar faculae,” *Mon Not R Astron Soc* **482**(4), 5290–5301 (2019).
- [8] Lean, J. L., Coddington, O., Marchenko, S. V., Machol, J., DeLand, M. T. and Kopp, G., “Solar Irradiance Variability: Modeling the Measurements,” *Earth and Space Science* **7**(8) (2020).
- [9] SOLANKI, S. K., SCHÜSSLER, M. and FLIGGE, M., “Secular variation of the Sun’s magnetic flux,” *Astron Astrophys* **383**(2), 706–712 (2002).
- [10] Eddy, J. A., “The maunder minimum,” *Science* (1979) **192**(4245), 1189–1202 (1976).
- [11] Gray, L. J., Beer, J., Geller, M., Haigh, J. D., Lockwood, M., Matthes, K., Cubasch, U., Fleitmann, D., Harrison, G., Hood, L., Luterbacher, J., Meehl, G. A., Shindell, D., Van Geel, B. and White, W., “Solar influences on climate,” *Reviews of Geophysics* **48**(4) (2010).
- [12] Usoskin, I. G., Arlt, R., Asvestari, E., Hawkins, E., Käpylä, M., Kovaltsov, G. A., Krivova, N., Lockwood, M., Mursula, K., O’Reilly, J., Owens, M., Scott, C. J., Sokoloff, D. D., Solanki, S. K., Soon, W. and Vaquero, J. M., “The Maunder minimum (1645-1715) was indeed a grand minimum: A reassessment of multiple datasets,” *Astron Astrophys* **581** (2015).
- [13] Lean, J. L., “Sun-Climate Connections,” [Oxford Research Encyclopedia of Climate Science], 1–55 (2017).
- [14] IPCC., “Climate Change 2021 Working Group I contribution to the Sixth Assessment Report of the Intergovernmental Panel on Climate Change Summary for Policymakers” (2021).
- [15] McCluney, W. R., [Introduction to Radiometry and Photometry, Second], Artech House, Boston (2014).
- [16] Datla, R. U. and Parr, A. C., [Introduction to Optical Radiometry] (2005).
- [17] Sapritsky, V. and Prokhorov, A., [Blackbody Radiometry], Springer (2020).
- [18] Carlesso, F., Rodríguez Gómez, J. M., Barbosa, A. R., Antunes Vieira, L. E. and Dal Lago, A., “Solar Irradiance Variability Monitor for the Galileo Solar Space Telescope Mission: Concept and Challenges,” *Front Phys* **10** (2022).
- [19] Kopp, G. and Lawrence, G., “THE TOTAL IRRADIANCE MONITOR (TIM): INSTRUMENT DESIGN,” *Sol Phys* **230**, 91–109 (2005).
- [20] Butler, J. J., Johnson, B. C., Rice, J. P., Shirley, E. L. and Barnes, R. A., “Sources of Differences in On-Orbital Total Solar Irradiance Measurements and Description of a Proposed Laboratory Intercomparison,” *J Res Natl Inst Stand Technol* **113**(4), 187–203 (2008).
- [21] Harber, D., Castleman, Z., Drake, G., Van Dreser, S., Farber, N., Heuerman, K. and Lehman, J., “Compact total irradiance monitor flight demonstration,” *CubeSats and SmallSats for Remote Sensing III*, 4–6, International Society for Optics and Photonics (2019).
- [22] Vaskuri, A. K., Stephens, M. S., Tomlin, N. A., Spidell, M. T., Yung, C. S., Walowitz, A. J., Straatsma, C., Harber, D. and Lehman, J. H., “High-accuracy room temperature planar absolute radiometer based on vertically aligned carbon nanotubes,” *Opt Express* **29**(14), 22533 (2021).
- [23] Feteira, A., “Negative temperature coefficient resistance (NTCR) ceramic thermistors: An industrial perspective,” *Journal of the American Ceramic Society* **92**(5), 967–983 (2009).
- [24] Vieira, L. E., “Brazilian Experimental Solar Telescope - Galileo Solar Space Telescope | GSST,” São José dos Campos (2014).
- [25] Vieira, L. E. A., Kopp, G., Dudok De Wit, T., da Silva, L. A., Carlesso, F., Barbosa, A., Muralikrishna, A. and Santos, R., “Variability of the Sun’s luminosity places constraints on the thermal equilibrium of the convection zone,” *Astrophys J Suppl Ser* **260**(2), 38 (2022).

- [26] Vieira, A. and Eduardo, L., “Galileo Solar Space Telescope Mission: A concept feasibility study,” 42nd COSPAR Scientific Assembly, E23, Pasadena (2018).
- [27] Carlesso, F., Vieira, L. E. A., Berni, L. A., Savonov, G. da S., Remesal Oliva, A., Finsterle, W. and de Miranda, E. L., “Physical and Optical Properties of Ultra-black Nickel–Phosphorus for a Total Solar Irradiance Measurement,” *Astrophys J Suppl Ser* **248**(1), 4 (2020).
- [28] Carlesso, F., Vieira, L. E. A., Berni, L. A. and Savonov, G. da S., “Design, Implementation and Characterization of Cavity for Absolute Radiometer,” *Front Phys* **9**, 52 (2021).
- [29] CPRIME, C. de P. I. de M. E., “Galileo Solar Space Telescope Mission Study Report,” Sao Jose dos Campos (2018).
- [30] Muralikrishna, A., Dos Santos, R. D. C. and Vieira, L. E. A., “Exploring possibilities for solar irradiance prediction from solar photosphere images using recurrent neural networks,” *Journal of Space Weather and Space Climate* **12**, 1–23 (2022).
- [31] Vieira, L. E. A., Lago, A., Rockenbach, M., Guarnieri, F. L., Da Silva, L. A., Carlesso, F., Alves, L. R., Souza, V. M. C. E. S. and Jauer, P. R., “Status of the Galileo Solar Space Telescope Mission(GSST) proposal,” AGU Fall Meeting Abstracts, SH13C-3447 (2019).
- [32] HUNSPERGER, R. G., [Integrated optics, Sixth Edit], Springer, New York (2009).
- [33] Razavi, B., [Design of Integrated Circuits for Optical Communications], Boston (2009).
- [34] Shirdel, M. and Mansouri-Birjandi, M. A., “Photonic crystal all-optical switch based on a nonlinear cavity,” *Optik (Stuttg)* **127**(8), 3955–3958 (2016).
- [35] TREYZ, G. V., “Silicon Mach–Zehnder waveguide interferometers operating at 1.3  $\mu\text{m}$ ,” *Conference on Lasers and Electro-Optics* **27**(2), 118–120, Optica Publishing Group (1991).
- [36] Camilo, M. E., Kassab, L. R. P., Assumpção, T. A. A., Cacho, V. D. D. and Alayo, M. I., “Fabrication and characterization of pedestal optical waveguides using TeO<sub>2</sub>-WO<sub>3</sub>-Bi<sub>2</sub>O<sub>3</sub> thin film as core layer,” *Thin Solid Films* **571**(P1), 225–229 (2014).
- [37] Heideman, R. G., Kooyman, R. P. H. and Greve, J., “Performance of a highly sensitive optical waveguide Mach-Zehnder interferometer immunosensor,” *Sens Actuators B Chem* **10**(3), 209–217 (1993).
- [38] Mina, A. M., Baez, H., Martins, G. S. P. and Alayo, M. I., “Development and fabrication of an optimized thermo-electro-optic device using a Mach-Zehnder interferometer,” *J Non Cryst Solids* **354**(19–25), 2565–2570 (2008).
- [39] Benaissa, K. and Nathan, A., “Silicon anti-resonant reflecting optical waveguides for sensor applications,” *Sens Actuators A Phys* **65**(1), 33–44 (1998).
- [40] Kozma, P., Kehl, F., Ehrentreich-Förster, E., Stamm, C. and Bier, F. F., “Integrated planar optical waveguide interferometer biosensors: A comparative review,” *Biosens Bioelectron* **58**, 287–307 (2014).
- [41] Prieto, F., Sepúlveda, B., Calle, A., Llobera, A., Domínguez, C. and Lechuga, L. M., “Integrated Mach-Zehnder interferometer based on ARROW structures for biosensor applications,” *Sens Actuators B Chem* **92**(1–2), 151–158 (2003).
- [42] Lean, J. L. and Rind, D. H., “How natural and anthropogenic influences alter global and regional surface temperatures: 1889 to 2006,” *Geophys Res Lett* **35**(18), 1–6 (2008).
- [43] Matthes, K., Funke, B., Andersson, M. E., Barnard, L., Beer, J., Charbonneau, P., Clilverd, M. A., Dudok De Wit, T., Haberreiter, M., Hendry, A., Jackman, C. H., Kretzschmar, M., Kruschke, T., Kunze, M., Langematz, U., Marsh, D. R., Maycock, A. C., Misios, S., Rodger, C. J., et al., “Solar forcing for CMIP6 (v3.2),” *Geosci Model Dev* **10**(6), 2247–2302 (2017).
- [44] Bomfim, F. A., Rangel, R. C., da Silva, D. M., Carvalho, D. O., Melo, E. G., Alayo, M. I. and Kassab, L. R. P., “A new fabrication process of pedestal waveguides based on metal dielectric composites of Yb<sup>3+</sup>/Er<sup>3+</sup> codoped PbO-GeO<sub>2</sub> thin films with gold nanoparticles,” *Opt Mater (Amst)* **86**(October), 433–440 (2018).
- [45] Bomfim, F. A., Da Silva, D. M., Kassab, L. R. P., De Assumpção, T. A. A., Del Cacho, V. D. and Alayo, M. I., “Advances on the fabrication process of Er<sup>3+</sup>/Yb<sup>3+</sup>:GeO<sub>2</sub>-PbO pedestal waveguides for integrated photonics,” *Opt Mater (Amst)* **49**, 196–200 (2015).
- [46] Carvalho, D. O., Kassab, L. R. P., Del Cacho, V. D., Silva, D. M. and Alayo, M. I., “A review on pedestal waveguides for low loss optical guiding, optical amplifiers and nonlinear optics applications,” *Journal of Luminescence journal* **203**(June), 135–144 (2018).
- [47] Carvalho, D. O. and Alayo, M. I., “Pedestal anti-resonant reflecting optical waveguides,” *Oxide-based Materials and Devices II* **7940**(March 2011), 2011 SPIE OPTO, Ed., 794017, San Francisco (2011).